

# Investigation of the Effect of Engine Speed on the Radial Inflow Turbine for Automotive Exhaust Energy Recovery

<sup>1</sup>Nwaji, G.N. <sup>++</sup>, <sup>1</sup>Udongwo, S., <sup>2</sup>Ajayi, K.T., <sup>1</sup>Nwifo, O.C., <sup>1</sup>Onwuachu, C.C., <sup>1</sup>Ofong, I.

<sup>1</sup>Federal University of Technology, P.M.B. 1526, Oweeri, Imo State, Nigeria

<sup>2</sup>University of Lagos, Akoka, Yaba, Lagos, Nigeria

<sup>++</sup> Corresponding Author: godswillmee@gmail.com

## Abstract

A computational fluid dynamic investigation of flow across a vaned single-entry radial inflow turbine coupled to an exhaust pipe of a 2.5L petrol engine was carried out to ascertain the extent of exhaust energy recoverability for driving the vehicle auxiliaries. A 3D model of the turbine cascade was developed, meshed and imported into Autodesk CFD. Appropriate boundary conditions for the simulation were specified assuming a 100% volumetric efficiency for the test engine at specified speeds. A steady non-pulsatile flow was modelled with volume flow rate inlet boundary condition while the outlet condition was specified as unknown in order to determine the properties of the flow and fluid spouting into the turbine from the engine. The SST  $k - \omega$  turbulence model and advanced Petrov – Galerkin's advection scheme were applied for the study. Results obtained provide insight to the variations of flow and fluid properties across the volute and outlet pipe at different engine speeds.

**Keywords:** Vaned Single-entry, Radial inflow turbine, Non-Pulsatile Flow, Numerical Simulation, Finite Volume, Computational Fluid Dynamics.

## 1.0 Introduction

It is common knowledge that the exhaust gas of internal combustion engines is a potential source of energy that can be recovered for a wide range of applications. About 30% of the total energy offered by the fuel is contained in the exhaust gases of these engines, while also roughly 30% is utilized as useful work [1, 8, 2, 3]. This energy appears in various forms, namely, fluid, kinetic and thermal. This allows a variety of methods for its recovery. The fluid coupled with the kinetic energy recovery has been the most investigated due to its offer of ease of energy recovery. This is inferred from the popularity of turbocharging or turbocompounding which employs a turbine for the energy extraction. Research works also exist for the various methods employed to recover the exhaust gas thermal energy [1, 4]. Since from thermodynamic concept, energy transfer or conversion is never 100 percent efficient, not all the energy contained in the exhaust gases can be recovered by the various recovery methods available just as it is with the internal combustion engine. Therefore, some have reported on the methods of improving the efficiencies of the various processes for energy recovery [5, 6, 7]. Mingyang et al [5] determined from both experimental and numerical analyses, an optimized volute geometry which proved to be better in all considerations than the counterpart geometry analyzed. Srithar and Ricardo [6] also determined by experimentally studying a variable geometry mixed flow turbine, that the variable geometry mixed flow turbine shows higher peak efficiency and swallowing capacity at various vane angle settings compared to an equivalent nozzleless turbine. Ajayi and Ojakovo [9] conceptualized the use of high kinetic energy automobile exhaust gas to power a micro turbine coupled to the vapour compression refrigeration system compressor for driving the air conditioner. They designed, constructed and tested the set-up and carried out preliminary thermodynamic analysis of the system which revealed a 17 percent improvement on engine power as against the conventional mechanical drive of the air conditioner compressor for compression ignition engines. They also reported a 2% decrease in effectiveness in the case of spark ignition engines at temperatures exceeding 1400K. However, they concluded that the proposed innovation would enhance primary energy diversification leading to fuel economy and improved engine performance, mostly in terms of longevity of the prime mover. Ajayi et al [10], numerically studied the properties of high energy gas flows through a micro turbine in 3D cascade. Flow properties variations across the exhaust outlet were computationally examined on the basis of gas dynamic analysis of theoretical engine cycles. The 2D flow structure in the cascade revealed that the available kinetic energy of the exhaust gas can be put to more meaningful use by the extraction of shaft work using the micro turbine. However, they suggested further work to ascertain the effect of variable engine speed on the proposed novelty. Therefore, this study employs optimized volute geometry of a vaned radial turbine coupled to a 2.5L petrol engine to analyze the variations of flow and fluid properties through the turbine at different engine speeds in order to ascertain the amount of energy recoverable from the exhaust gas for driving vehicle auxiliaries.

**2.0 Methodology**

**2.1 Geometric Model**

A geometric model of the single-entry vaned turbine geometry was developed based on the information obtained from Garrett turbocharger manufacturer catalogue. With the 2.5L engine capacity and 130kW rated power, the turbocharger’s dimensions were selected from the catalogue. The section of the turbine-volute-outlet pipe assembly used for the study is as shown Fig. 1.

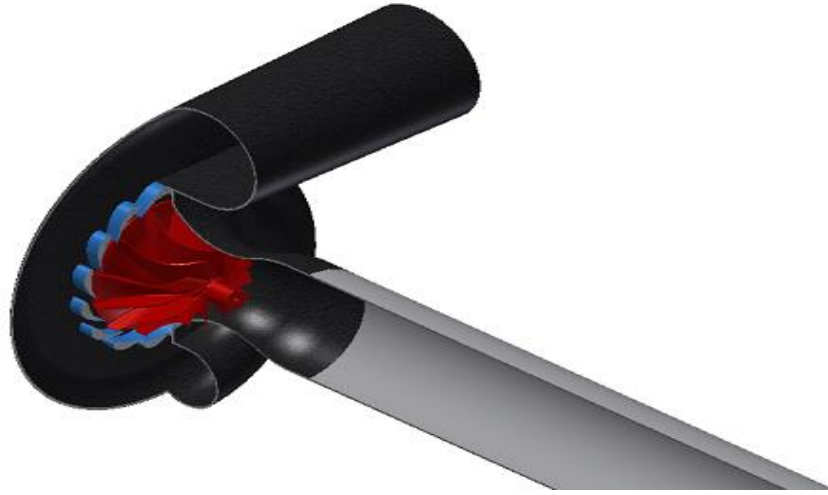


Fig 1: Section of turbine-volute-outlet pipe assembly

The geometry was designed with Autodesk Inventor, treated for areas that may cause meshing errors and exported to the Autodesk CFD software. The inlet boundary condition was set at steady volume flow rate but varied at different engine speeds. The outlet condition of the exhaust pipe was set as unknown since the outlet pipe was not sufficiently long enough to specify a zero bar gauge pressure. The unknown boundary condition allows the software to compute the flow and fluid conditions at such flow terminal. A rotating region boundary condition was specified for a rotating region afore created in the CAD model.

**2.1.1 Computational mesh**

In order to reduce computation time, automatic mesh generation was carried out with no refinements done. This resulted in a sufficient mesh element distribution and density to capture the flow as shown in Fig. 2. There are a total of 123,213 nodes and 435,224 elements in the whole turbine stage including the exhaust pipe.

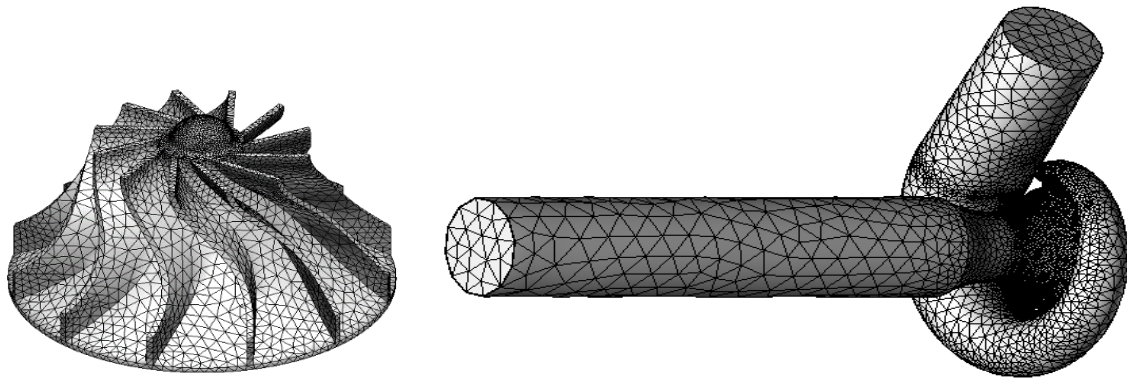


Figure 2: Mesh distribution

**2.2 Governing equations**

The governing equations for the computation of are those of the continuity, momentum and energy, given respectively as:

$$\frac{\partial \rho}{\partial t} + \vec{\nabla} \cdot (\rho \vec{V}) = 0 \tag{1}$$

$$\frac{\partial(\rho \vec{V})}{\partial t} + \vec{\nabla} \cdot (\rho \vec{V} \vec{V}) = \rho \vec{g} + \vec{\nabla} \cdot \sigma_{ij} \tag{2}$$

$$\rho u \frac{\partial e}{\partial x} + \rho v \frac{\partial e}{\partial y} = \frac{\partial}{\partial x} \left( k \frac{\partial T}{\partial x} \right) + \frac{\partial}{\partial y} \left( k \frac{\partial T}{\partial y} \right) - P \left( \frac{\partial u}{\partial x} + \frac{\partial v}{\partial y} \right) + \mu \phi + \dot{q} \quad 3$$

where

$$\mu \phi = \mu \left\{ \left( \frac{\partial u}{\partial y} + \frac{\partial v}{\partial x} \right)^2 + 2 \left[ \left( \frac{\partial u}{\partial x} \right)^2 + \left( \frac{\partial v}{\partial y} \right)^2 \right] - \frac{2}{3} \left( \frac{\partial u}{\partial x} + \frac{\partial v}{\partial y} \right)^2 \right\} \quad 4$$

The Shear Stress Transport  $k - \omega$  (SST  $k - \omega$ ) or Menter's  $k - \omega$  turbulence model was used to model turbulence which is suited to such flow analysis as compressible flow through turbomachines. The mathematical representation is given as:

$$\frac{\partial(\rho k)}{\partial t} + \frac{\partial(\rho u_j k)}{\partial x_j} = P - \beta^* \rho \omega k + \frac{\partial}{\partial x_j} \left[ (\mu + \sigma_k \mu_t) \frac{\partial k}{\partial x_j} \right] \quad 5$$

$$\frac{\partial(\rho \omega)}{\partial t} + \frac{\partial(\rho u_j \omega)}{\partial x_j} = \frac{\gamma}{v_t} P - \beta \rho \omega^2 + \frac{\partial}{\partial x_j} \left[ (\mu + \sigma_\omega \mu_t) \frac{\partial \omega}{\partial x_j} \right] + 2(1 - F_1) \frac{\rho \sigma_{\omega 2}}{\omega} \frac{\partial k}{\partial x_j} \frac{\partial \omega}{\partial x_j} \quad 6$$

The advection scheme used is based on the modified Petrov-Galerkin method which is a mathematical method used to obtain approximate solutions of partial differential equations which contain terms with odd order.

### 3.0 Results and Discussion

The variations of properties for the various flows through the vanes at an engine speed of 5000rpm are as shown in Figs 3a-g.

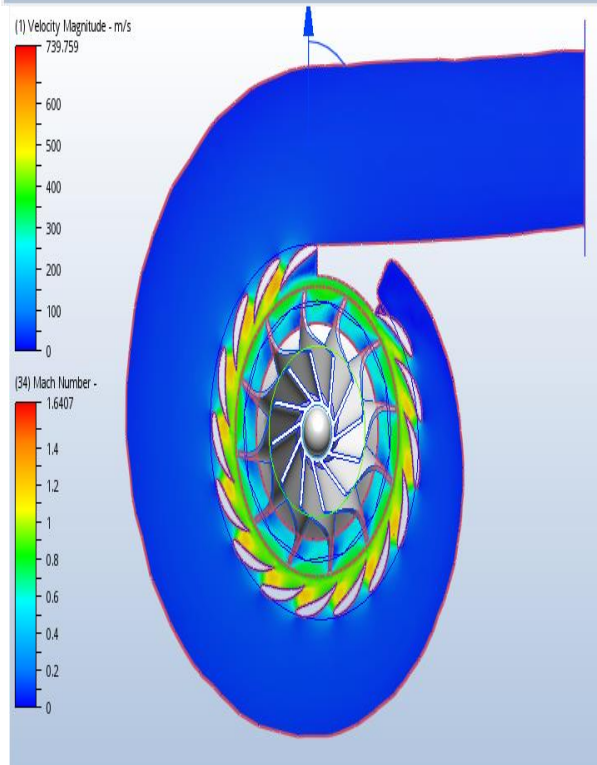
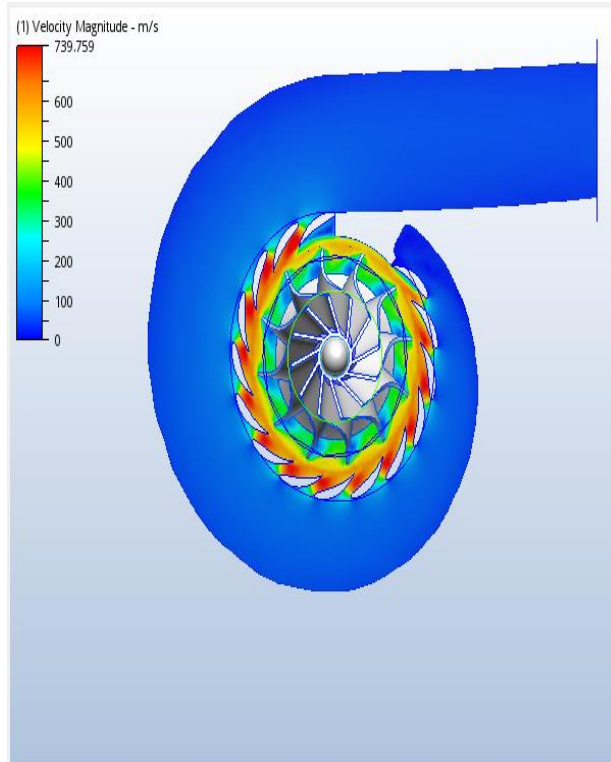


Fig.3a Velocity across turbine vanes

Fig.3b Mach Number across turbine vanes

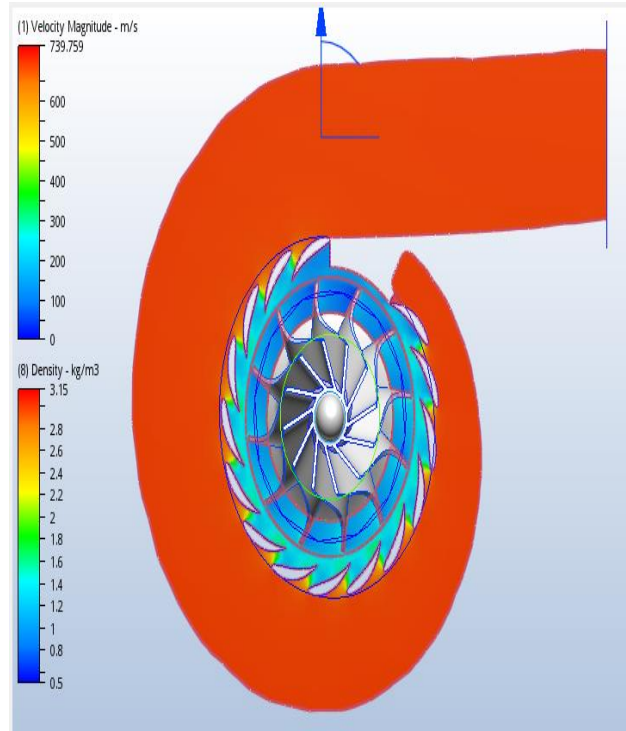


Fig.3c Density across turbine vanes

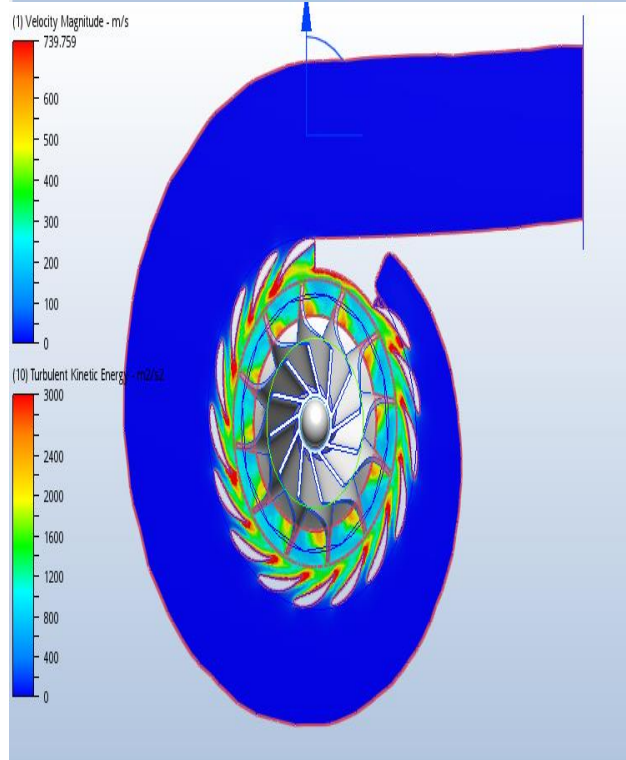


Fig.3d TKE across turbine vanes

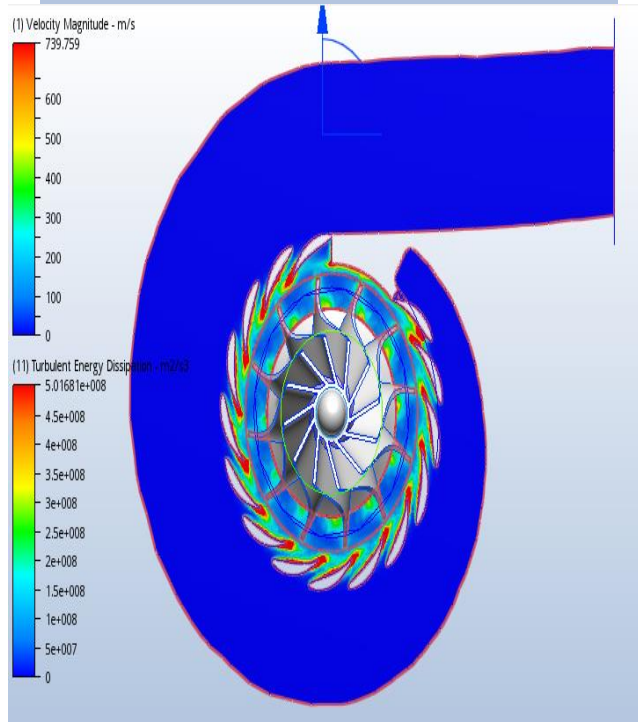
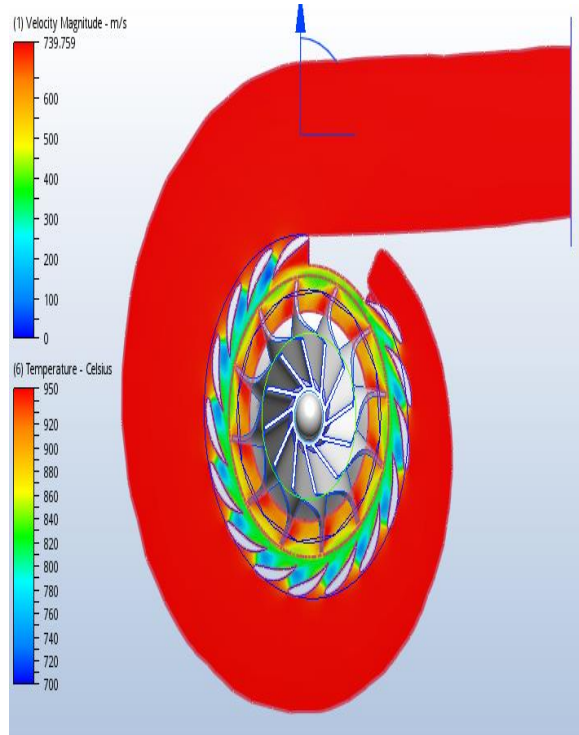


Fig.3e Temperature across turbine vanes

Fig.3f TED across turbine vanes

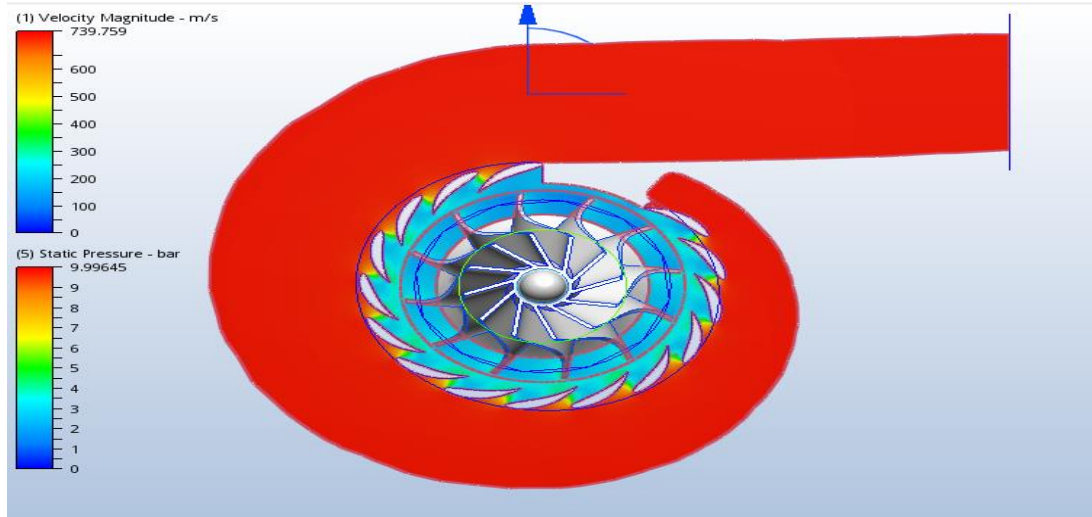


Fig.3g Variation of static pressure across the turbine vanes

It is observed that a distinct change in flow properties occurred in the vaned region of the volute. From the velocity and Mach number contour plots, it is seen that flow is accelerated in the vaned region. This is due to the fact that the vanes are arranged to serve as nozzles. This results in a decrease in the fluid density, temperature and the static pressure. It can also be observed that there was an increase in the turbulence kinetic energy and turbulent energy dissipated with maximum values occurring at the tip of the vanes.

Table 1 shows the fluid properties at the inlet to the turbine and outlet from the exhaust pipe at different engine speeds while Figs.4a-c show the corresponding Static Pressure, Density and Temperature variations with engine speeds from the turbine inlet and to the exhaust outlet.

Engine Speed (rpm)	Pressure (Gauge) (bar)			Density (kg/m <sup>3</sup> )			Temperature (K)		
	Inlet	Outlet	$\Delta P_{tot}$	Inlet	Outlet	$\Delta \rho_{tot}$	Inlet	Outlet	$\Delta T_{tot}$
2000	0.079	0.0178	0.0611	0.3427	0.3235	0.0192	800	800	0
3000	0.180	0.0399	0.1398	0.3577	0.3158	0.0418	850	849.64	0.365
4000	0.660	0.1747	0.4855	0.4809	0.3414	0.1385	900	898.51	1.49
5000	9.786	1.0002	8.7862	2.9765	0.5674	2.4091	950	921.87	28.13
6000	30.58	2.7556	27.8244	8.3651	1.0489	7.3162	1000	937.30	62.70

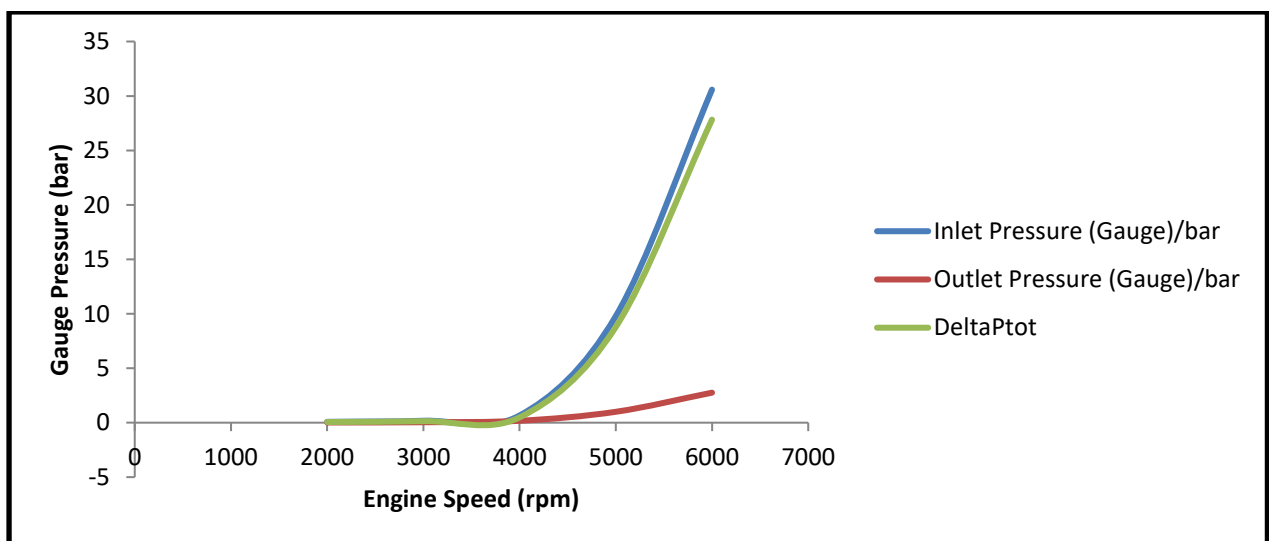


Fig.4a Variation of Pressure with Engine Speed across the turbine

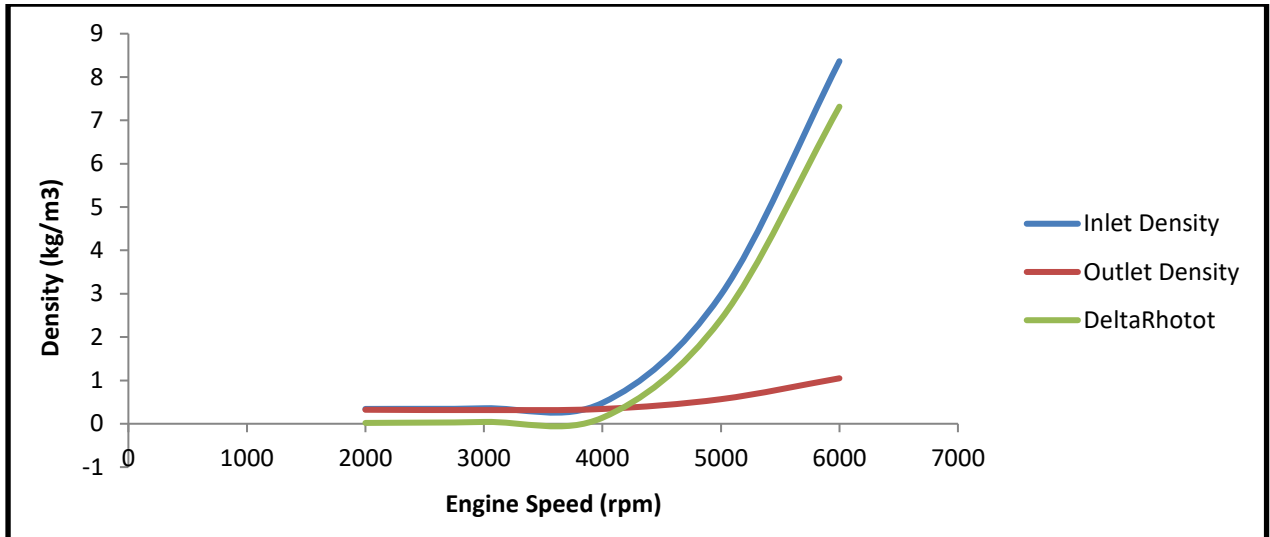


Fig.4b variation of Density with Engine Speed across the turbine

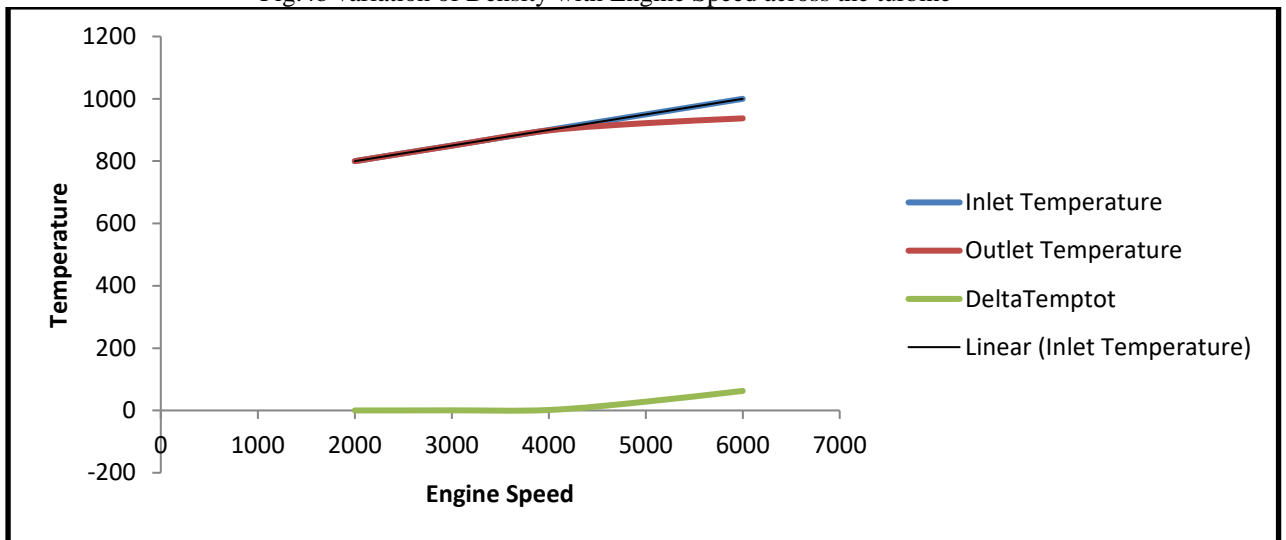


Fig.4c Variation of Temperature with Engine Speed across the turbine

The profiles show that at low engine speeds, pressure and temperature drops are not very significant. Significant drops are noticed for engine speeds above 5000rpm with a pressure drop of as high as 8bar and temperature drop of 28.13°C for an engine speed of 5000rpm. Fig. 5 shows the planes cutting through the outlet pipe from the turbine outlet to the exhaust outlet while Figs 6a-j show the variations of flow properties across the planes cutting through the outlet pipe at different engine speeds.

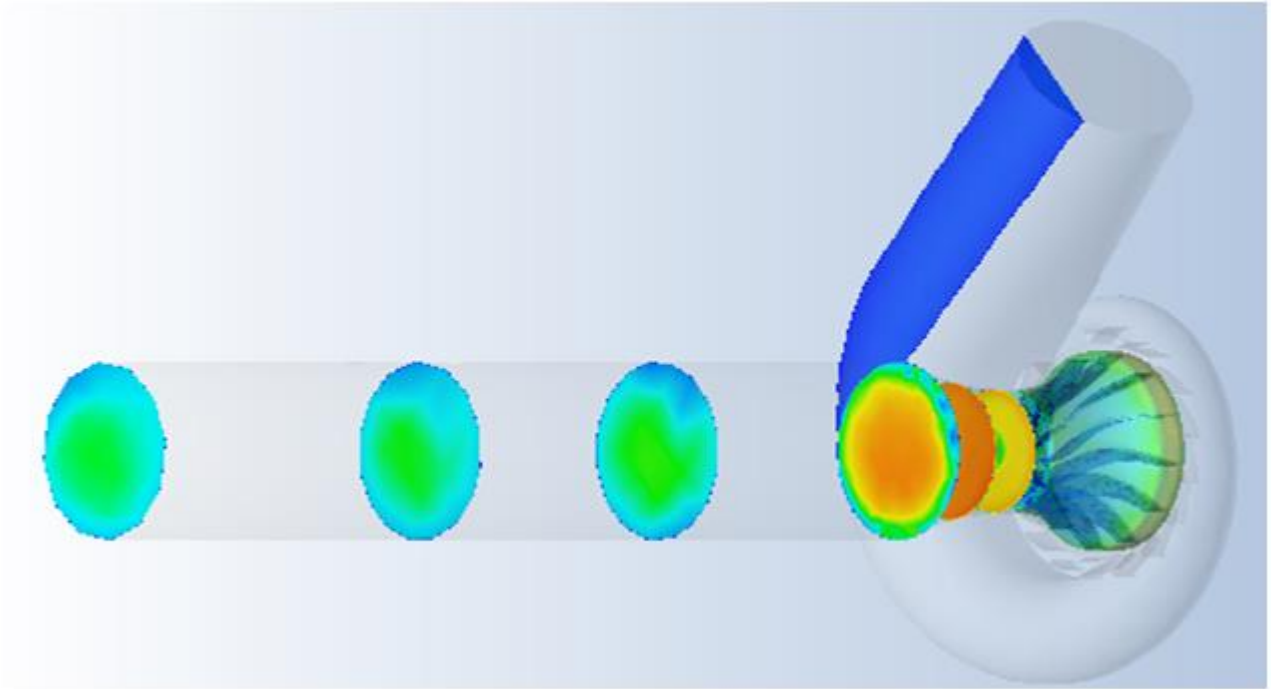


Figure 5: Z\_perp\_# analysis planes

The Z\_perp\_# corresponds to planes perpendicular to the axis of rotation, the Z-axis. The planes in the images are numbered Planes 1 to 6 from left to right, and the flow properties variations taken at specified planes are as shown in Figs 6a-j.

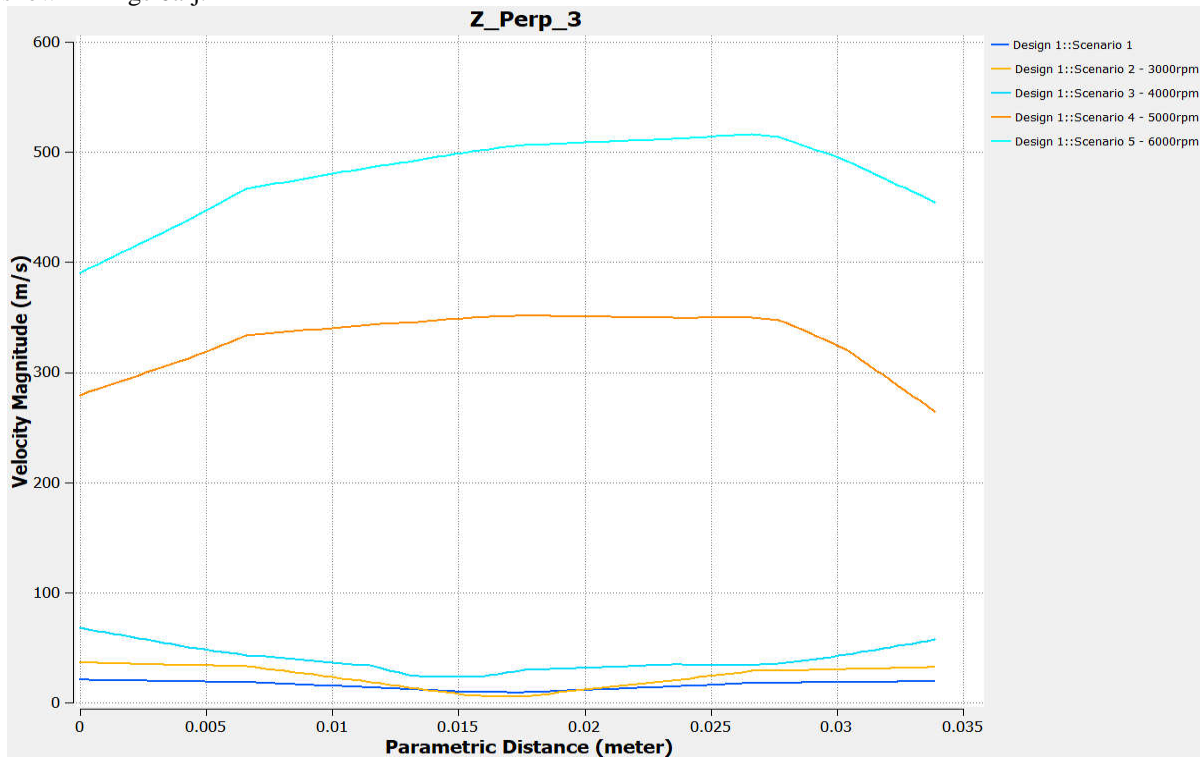


Fig.6a Variation of Velocity across the outlet pipe at different engine speeds

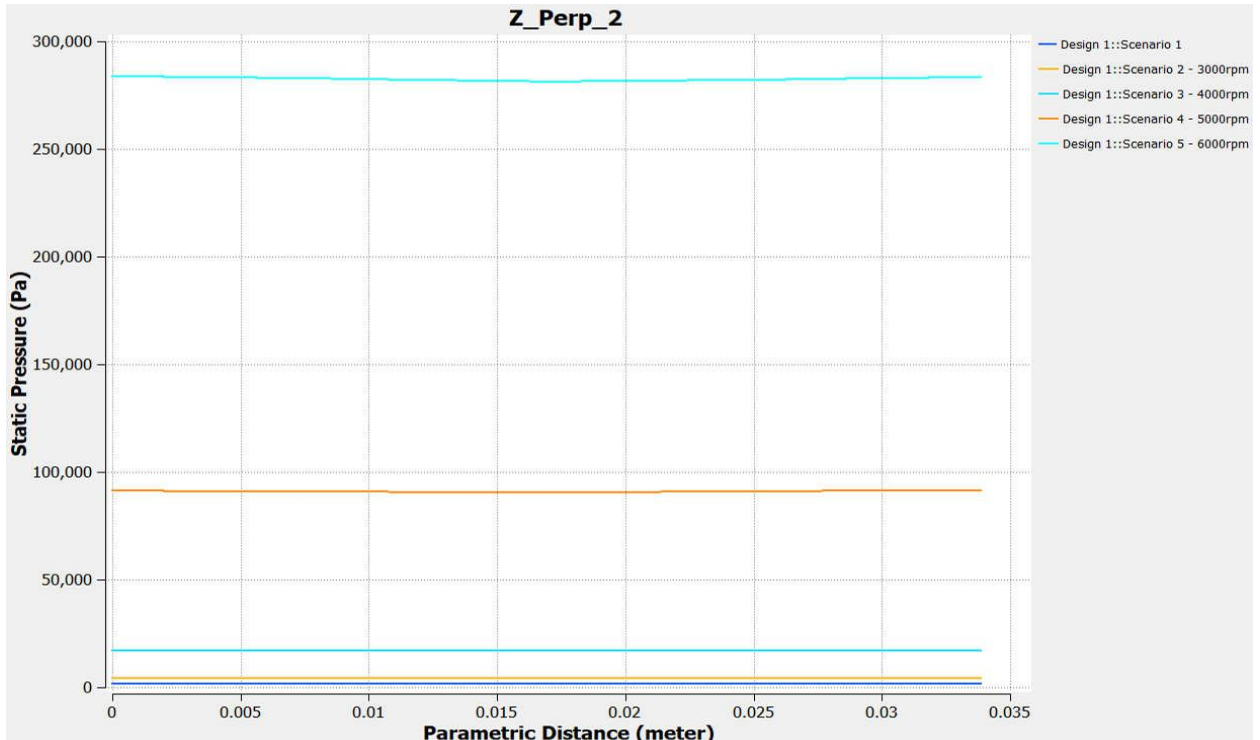


Fig.6b Variation of Static Pressure across the outlet pipe at different engine speeds

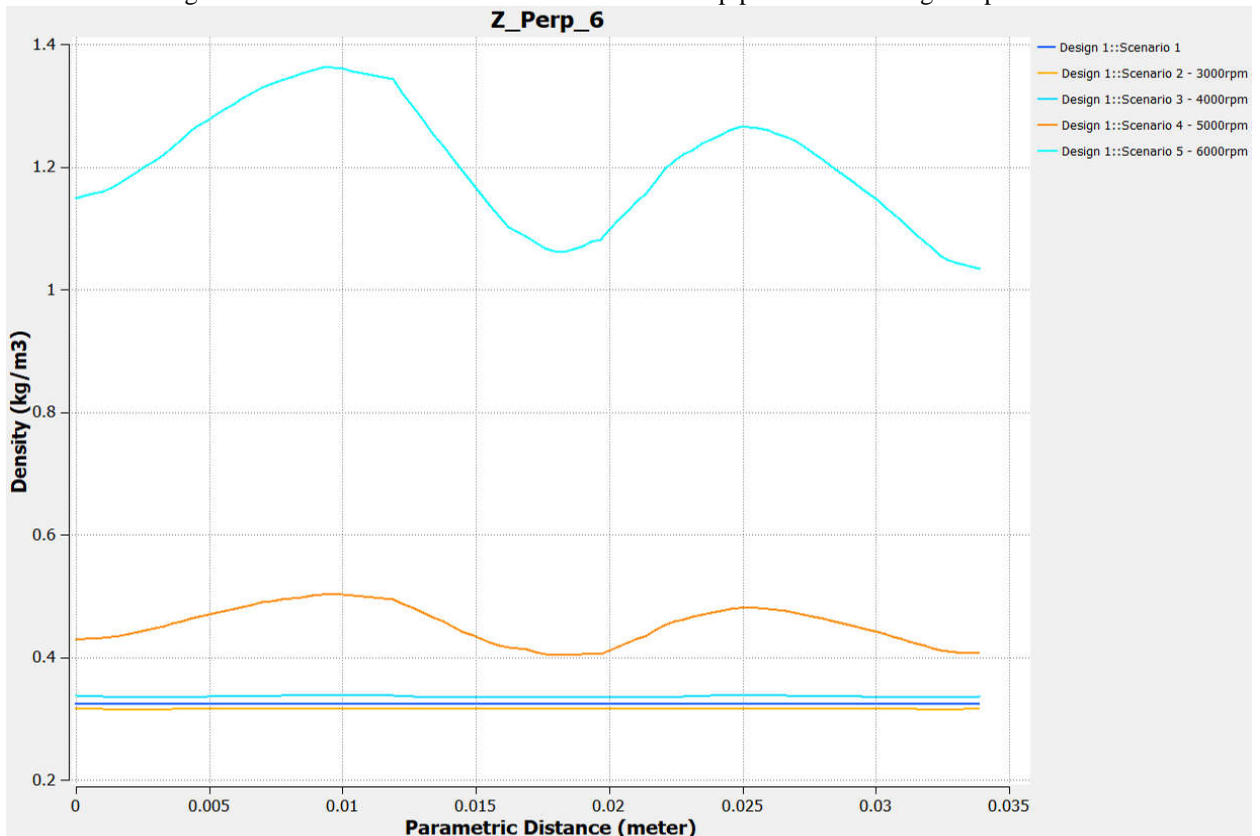


Fig.6c Variation of Density across the outlet pipe at different engine speeds

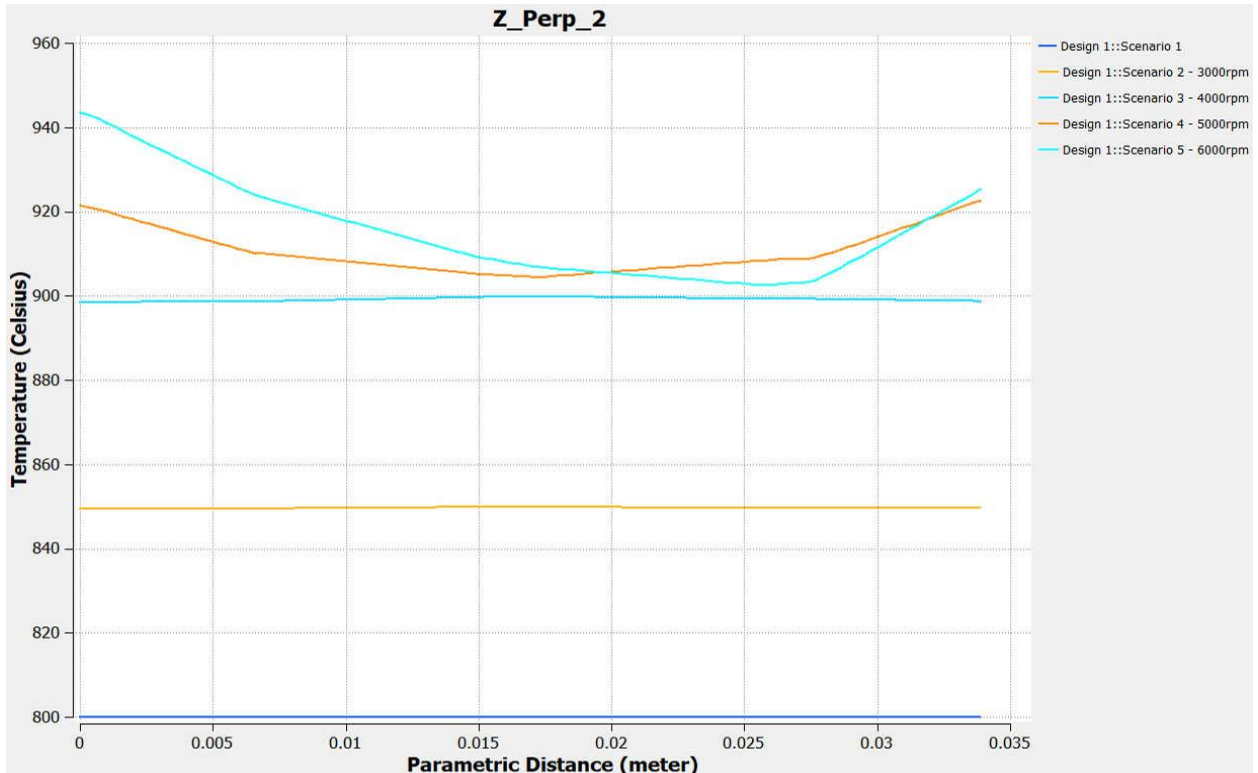


Fig.6d Variation of Temperature across the outlet pipe at different engine speeds

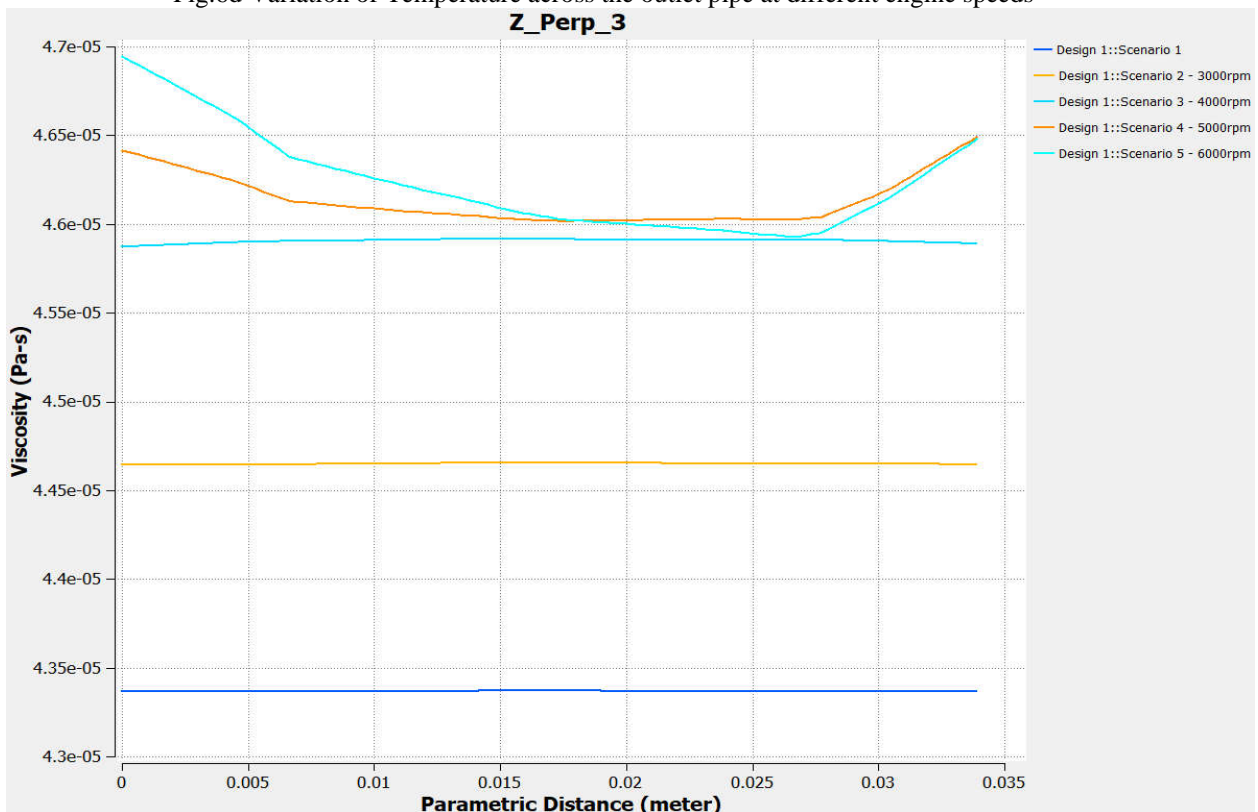


Fig.6e Variation of Viscosity across the outlet pipe at different engine speeds

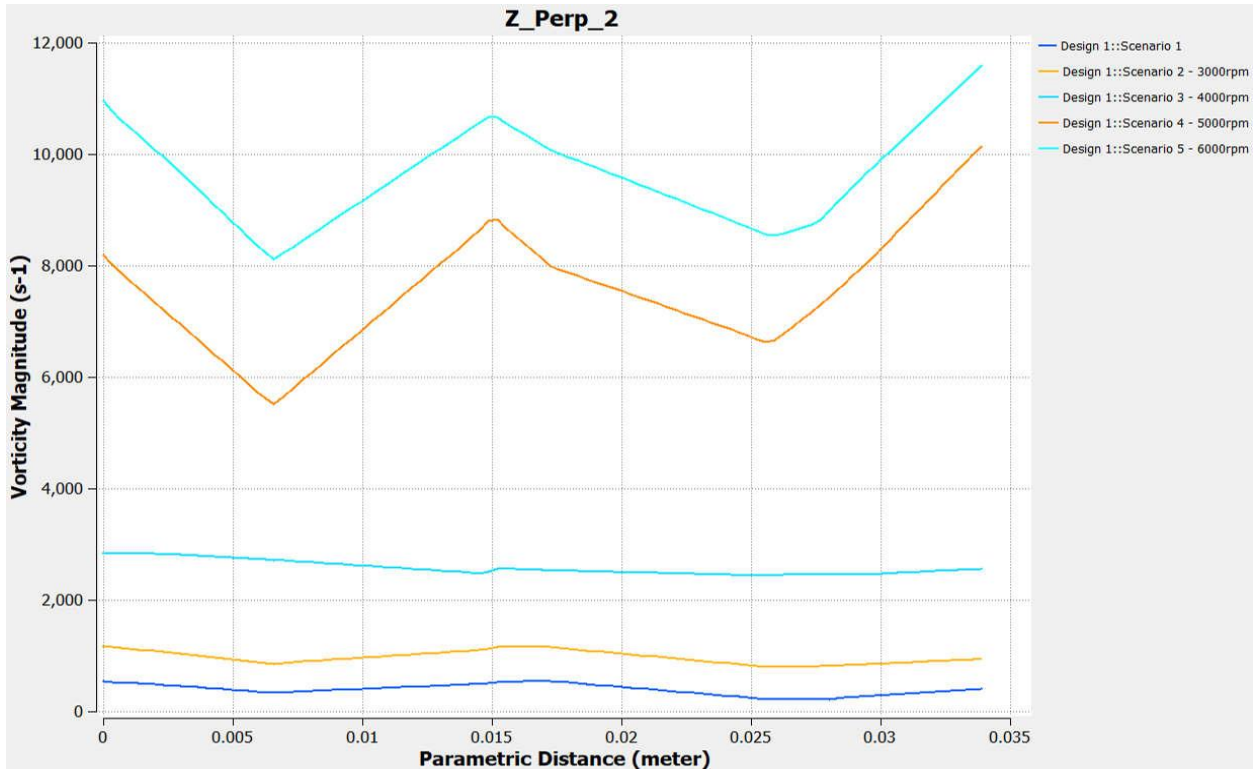


Fig.6f Variation of Vorticity across the outlet pipe at different engine speeds

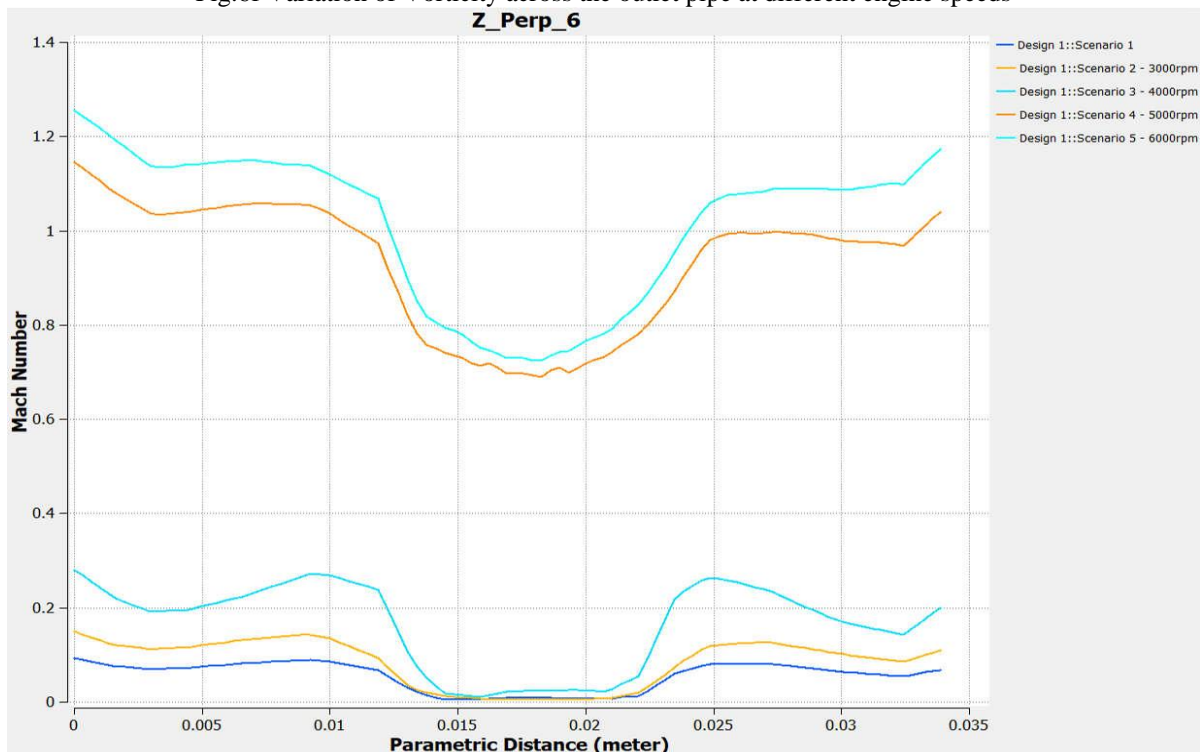


Fig.6g Variation of Mach Number across the outlet pipe at different engine speeds

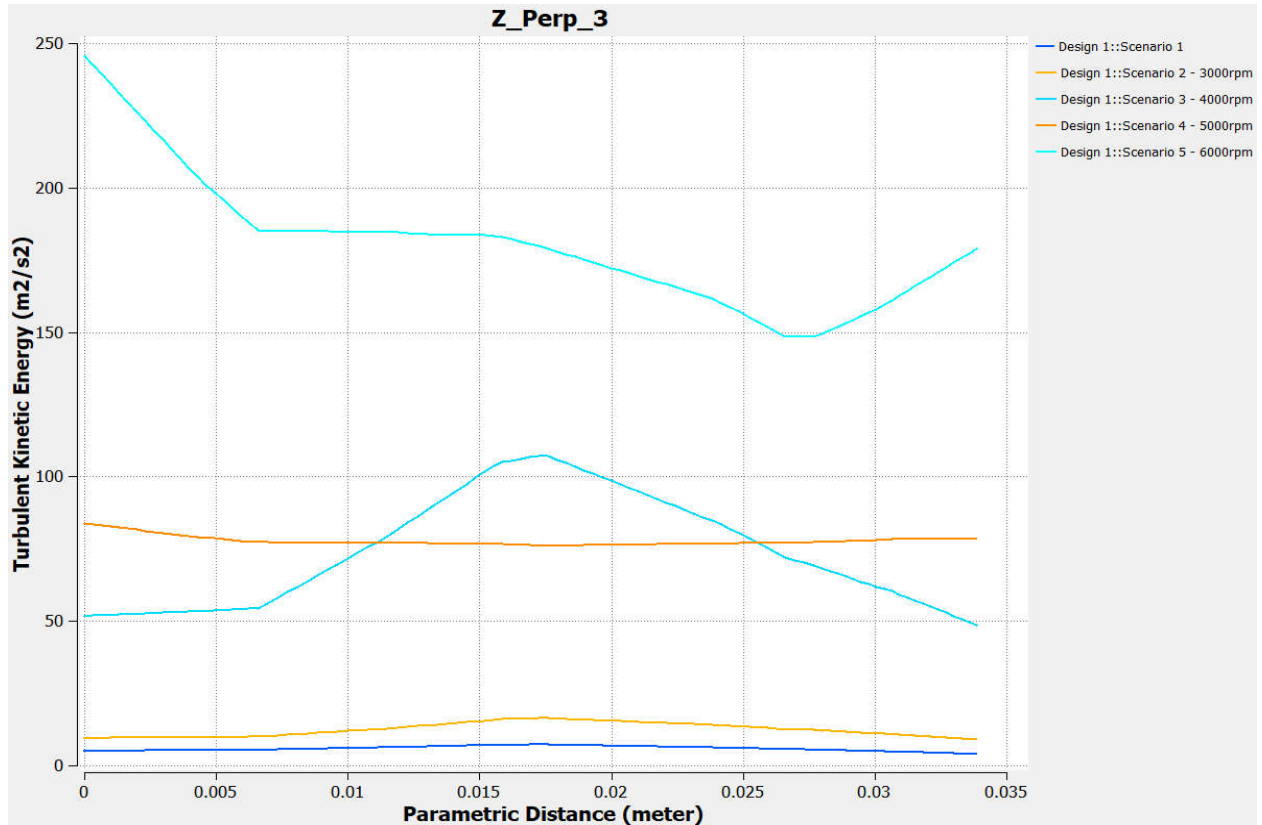


Fig.6h Variation of TKE across the outlet pipe at different engine speeds

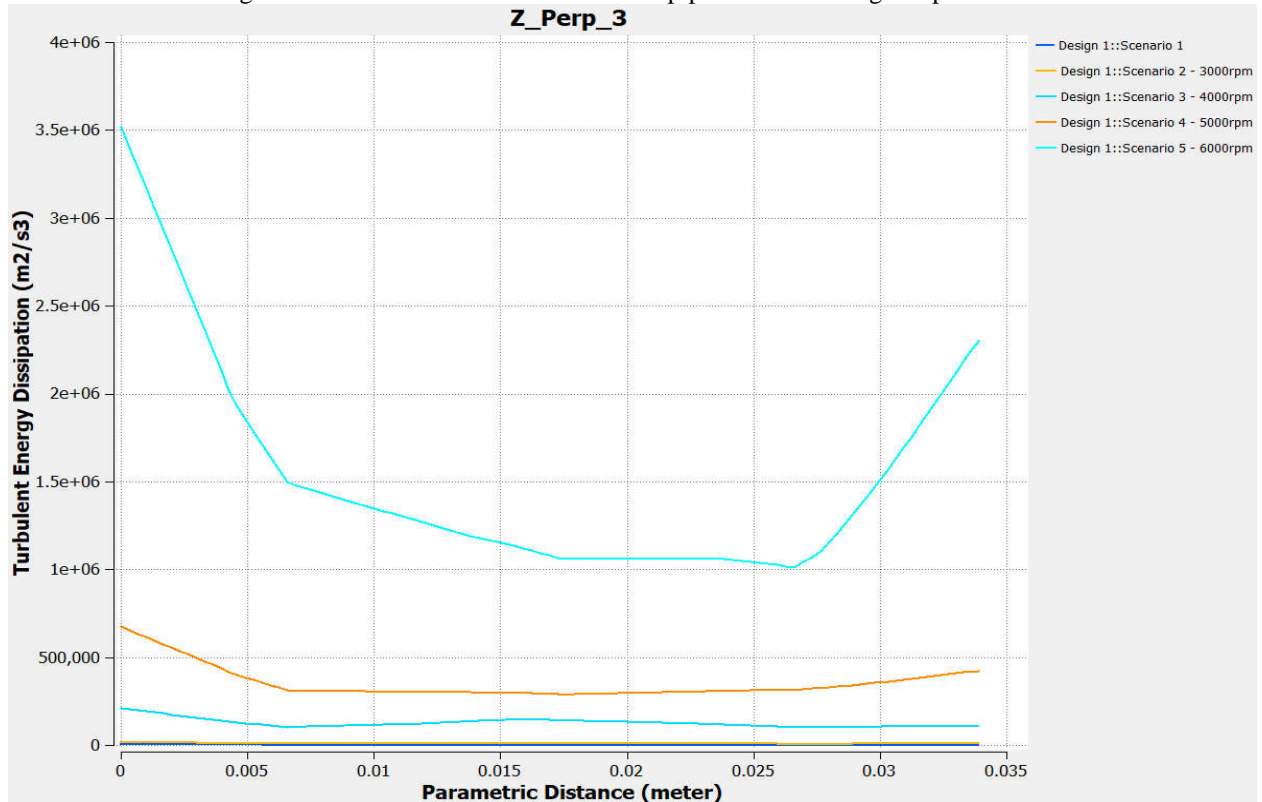


Fig.6i Variation of TED across the outlet pipe at different engine speeds

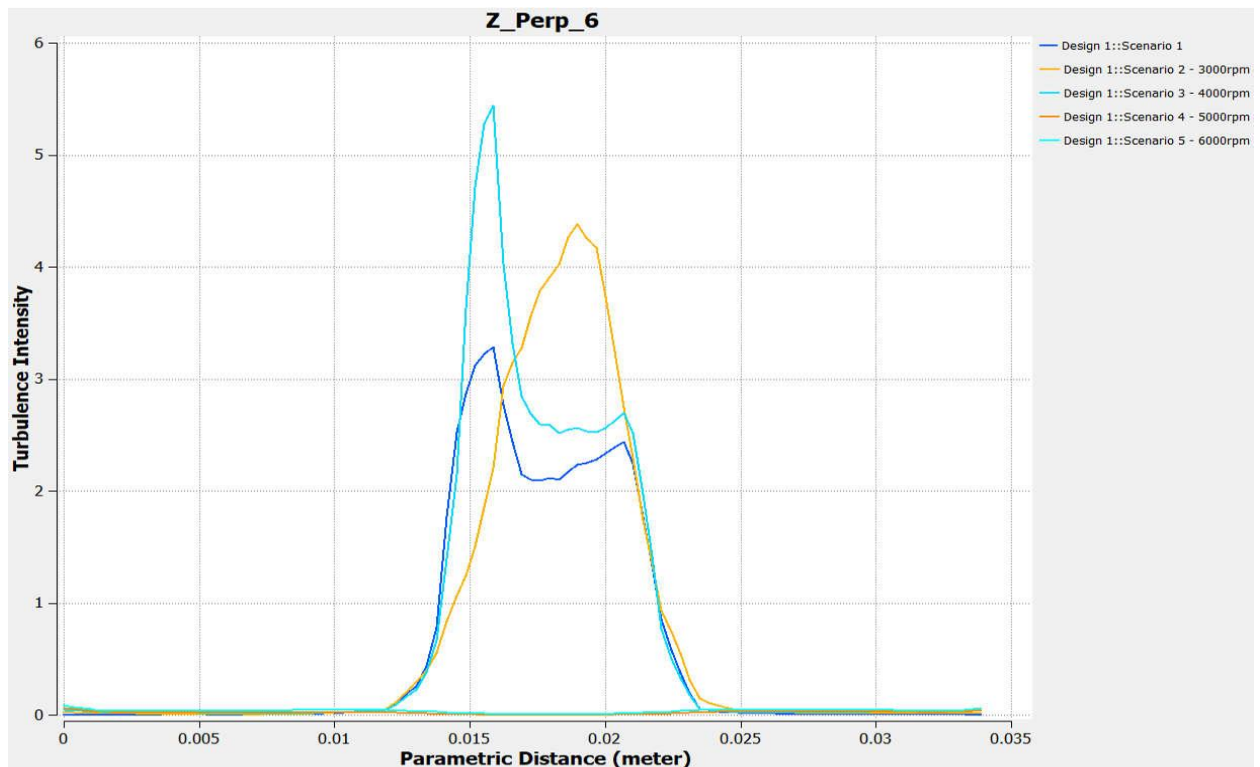


Fig.6j Variation of Turbulence Intensity across the outlet pipe at different engine speeds

Plane 6 corresponds to the plane which defines the cross sectional area of the volute just a little away from the turbine while plane 1 corresponds to the cross-section of the exhaust outlet. All other planes 2, 3, 4, and 5 are in between the exhaust outlet and the volute outlet. The property variations are assumed symmetrical and hence, analysis is done from left to the middle. Firstly, the gradual increase in velocity from left to right of the velocity profile is as a result of the no slip condition which was a boundary condition in the analysis. This relates to an increase in pressure and density and a reduction in temperature and viscosity. Vorticity also reduces in this region.

The second region of reducing velocity is primarily attributed to flow separation which occurs in the turbine. This causes the velocity just close to the mid-axis of the turbine to be very low and virtually zero for low volumetric flows. The second region of reducing velocity can also be attributed to the nature of the flow, vortex flow due to the blade angles. This flow characteristic causes a reduction in pressure as we move towards the mid axis. This drop in pressure results in an increase in the temperature which is also due to the fact that the conditions in this region are almost stagnation conditions. For low volume flow rates, much variation in properties cannot be observed. For higher volume flow rates, a distinct variation in properties can be observed.

The Mach Number as is seen for the first three volume flow rates is low while for higher volume flow rates, the  $Ma$  is a little above one. The former implies that for lower volumetric flows, the flow is not choked at the throat since the flow out of the diverging section is subsonic with a very low  $Ma$ . For higher values of volume flow rate however, it is observed that the flow out of the diverging section of the nozzle which contains the turbine is supersonic. This is corroborated by the supersonic bulk value of the  $Ma$  for that plane. This implies that the flow is choked at the throat.

Moving along the Z-axis, the next plane we encounter is plane 5 and plane 4 which corresponds to the image titled  $Z\_perp\_5$  and  $Z\_perp\_4$  respectively. This represents the mid-plane between the volute outlet and Plane 6. Along these planes, the velocity profile is seen to be displaying what resembles a laminar flow profile for high engine speeds while some unevenness in flow still exist for low volume flow rates. This may be due to the fact that the boundary layer is larger for low speed flows. The  $Ma$  for low volumetric flows still remain well below compressible. For an engine speed of 5000rpm however, the  $Ma$  just lies below the sonic,  $Ma$ . This implies that the flow for this engine speed is choked at the throat, since for the plane 6, the  $Ma$  in some regions was above sonic velocities. It continues subsonic after the throat. For an engine speed of 6000rpm however, the flow is choked and continues as supersonic at the diverging section of the volute to the exit with cross sectional area defined by Plane 4. The temperature profile for the first three engine speeds 2000, 3000 and 4000rpm are observed to remain roughly constant and equal to the total temperature. This is because of the assumption that the flow is adiabatic due to small heat transfer area. For higher velocities however, the temperature is observed to drop drastically toward the mid-axis of the plane. This is as expected for supersonic flows in a diverging nozzle. This leads to a corresponding increase as is seen in Plane 5. Density follows suit in the increase. At

Plane 4 however, which is just at the plane of exit from the diverging section into the outlet duct, the pressure and density dropped a little with a corresponding increase in the temperature.

For the low volumetric flows, the properties remain relatively constant. For the high volumetric flows however, velocity and Mach number continued reducing in the duct with a corresponding increase in temperature and reduction in static pressure and density. The temperature profile just at the exit plane still slopes down a little as a result of the no slip condition at the walls. This is also observed in the velocity profile with velocity increasing to a maximum at the mid-axis of the plane.

### Conclusion

A single-entry vaned turbocharger, coupled to a 2.5 L engine has been used for a computational fluid dynamic investigation of flow properties across the radial inflow turbine of the turbocharger in order to ascertain the effect of engine speed on the properties of the flow and hence postulate if the available shaft power from the turbine can drive the vehicle auxiliaries given the presence of back pressure in turbo-charging. It was observed that the Mach numbers at the outlet of the volute for high engine speeds were well in the supersonic region. From gas dynamics concept, nozzles are designed so that sonic conditions just occur at the throat. Any increase in the stagnation properties did not increase the mass flow rate but causes a buildup of pressure, which is the well known infamous problem of back pressure. This analysis therefore gives information on the possible engine speed range for which this can occur. The analysis can be further extended to various turbine sizes and configurations so that a family of curves can be obtained which will aid in the selection of turbochargers for various engines.

### References

- [1] L. A, G. Ludovic, D. Mouad, Z. Hamid, L. Vincent, Comparison and Impact of Waste Heat Recovery Technologies on Passenger Car Fuel Consumption in a Normalized Driving Cycle, *Energies* (2014), pp. 1-18.
- [2] F. Hellstroem, Numerical Computations of the Unsteady Flow in Turbochargers, Royal Institute of Technology, Stocholm, Sweden, 2010
- [3] S.J. Jadhao and G.D. Thombare, Review on Exhaust Gas Heat Recovery for Internal Combustion Engines, *International Journal of Engineering and Innovative Technology (IJEIT)*, vol. 2, no. 12, (2013)
- [4] M. Abidat, M. Hachemi, M. Hamel and M. K. Hamidou, Design and Flow Analysis of Radial Flow Turbines, *European Conference on Computational Fluid Dynamics, Algérie*, 2006.
- [5] Y. Mingyang, M.B. Ricardo, S. Rajoo, Y. Takao and S. Ibaraki, An investigation of volute cross-sectional shape on turbocharger turbine under pulsating conditions in internal combustion engines, *Energy Conversion and Management*, (2015) pp. 1-11.
- [6] R. Srithar and M.B. Ricardo, Variable Geometry Mixed Flow Turbine for Turbochargers, *International Journal of Fluid Machinery and Systems*, vol. 1, no. 1 (2008), pp. 1-14.
- [7] A.R. Tough, M. Tousei and J. Ghafari, Improving of the micro-turbine's centrifugal impeller performance by changing the blade angles, *ICCES*, vol. 14, no. 1 (2010), pp. 1-22.
- [8] L. Arnaud, G. Ludovic, D. Mouad, Z. Hamid, & L. Vincent, Comparison and Impact of Waste Heat Recovery Technologies on Passenger Car Fuel Consumption in a Normalized Driving Cycle, *energies* (2014) 1-18.
- [9] K.T. Ajayi, A.E. Ojakovo, Design and Development of Micro-Turbine Coupled Compressor for Air-Conditioning System in Automobiles, *Journal of Emerging Trends in Engineering and Applied Sciences (JETEAS)* 3 (2) (2012) 259-264.
- [10] K. T. Ajayi, G. N. Nwaji and O. B. Ojo., Numerical Study of the Properties of High Energy Gas Flow through a Micro-turbine in 3d Cascade, *Journal of Emerging Trends in Engineering and Applied Sciences (JETEAS)* 5(7) (2014) 88-94.